

Improved Rover Mobility Over Loose Deformable Slopes through Active Control of Body-Rotating Mechanism

Shipeng Lv, Yuntian Zhao, Zhenyang Chen, Chengyuan Gao, Longteng Hu, and Zhenzhong Jia*

Abstract—Changing the center of mass (COM) by adjusting rover’s posture is a commonly used design and control strategy to improve its mobility over sandy slopes. Different from traditional passive/active suspension system and wheel-leg designs, we use a novel rover design for improved sloped mobility over soft terrains. Our rovers consist of a mobile base (with differential suspension), a main body, and a 2-degree-of-freedom (2-DOF) body-rotating mechanism that can change the pose of the main body relative to the mobile base. By taking full advantage of the main body weight which accounts for most of the robot weight, we can effectively adjust the rover COM and load distributions for improved mobility. Based on mechanics analysis, the wheel-load model and terramechanics model, we propose a control strategy for slope climbing and traversing tasks. When given input information such as slope angle and travel direction, the control algorithm can adjust the rover posture for optimal mobility over slopes. Experimental results indicate that the proposed design and control strategy can effectively improve the rover mobility performance (improved traction, reduced slippages) over soft sloped terrains.

I. INTRODUCTION

Robotic explorations are becoming popular for scientific explorations in harsh environments such as Mars/lunar surfaces, hilly areas, and deserts, where the robot’s off-road mobility is an important mission-critical factor [1]. In these tasks, the site to be explored are often hilly or sloped areas covered with soft deformable soils. This is especially true for planetary explorations or volcanic field studies. The robots such as Mars/Lunar rovers need to explore the volcanic and meteorite craters, in order to study the internal structure and the mineral compositions of the planet, or search for elements (e.g., water) that can sustain life. Unfortunately, it can be very challenging for these rovers to traverse over these soft sloped terrains, due to wheel sinkage and slippages. Therefore, improving the rover mobility over soft slopes through novel mechanisms, controls, and planning algorithms are becoming very critical for scientific explorations [1].

A. Related Work

This paper focuses on using mass-moving mechanism that can adjust the rover’s COM (center-of-mass) and wheel load to improve its mobility over soft sloped terrains. In the sequel, we review some related work from the literature.

Articulated or active suspensions are often used to enhance the rover’s off-road mobility, including sloped mobility. For

example, one can use linear actuators to adjust the height of suspension arms (rocker links) in [2] [3], thereby changing the COM and wheel load distributions for improved slope climbing and traversing over loose soils. Similar work has also been reported in [4], where an active rotating suspension is used to adjust the COM and force distributions.

Individual suspension or wheel-leg mechanism can further improve sloped mobility by taking advantage of increased operation modes and control authorities. A wheel-leg design that can change the ground contact points and COM has been reported in [5]. Ref. [6] combines individual active suspension with wheel modules to execute unconventional gaits to facilitate locomotion over challenging hilly granular terrains. However, wheel-leg mechanism requires more actuators and complicated planning/control algorithms [7].

The main body accounts for most of the robot weight due to the mounted power, navigation, communication, control, and scientific payload. One limitation of many active suspension or wheel-leg designs reported in the literature is that the main body is not used for mass-shifting purposes; i.e., it acts as dead weight. Ref. [7] proposes a novel design, which adjusts the robot’s attitude and wheel loads through the roll and pitch operations of the main body. The experiments show that the design can effectively improve the rover’s stair and slope climbing ability over solid/hard surfaces. Its mobility on soft deformable terrain has not been evaluated.

B. Innovation and Contributions of This Paper

With inspiration from the literature, we focus on the design and control of body-rotating mechanism (see Fig.2), and the evaluation of its climbing/traversing abilities over soft sloped surfaces in this paper. The main contributions are:

- Developed two rovers with body-rotating mass-moving mechanisms that can actively adjust the rover’s COM and wheel loads to improve the sloped mobility.
- Based on mechanics analysis, developed control strategy that can optimize the body servo angles when given slope angles and heading direction, so that the rover can even wheel loads for maximum mobility.
- Evaluated the the proposed design and its mobility in sloped soft terrain (both climbing and traversing).

The remainder of this paper is organized as follows. Section II-A illustrates the robot platform with body-rotating mechanisms. Section III presents the mechanics analysis and control strategy development. Section IV verifies the proposed approach through experimental investigations of the rover’s slope climbing and traversing performances. Section V shows the conclusion and future work.

The authors are with Shenzhen Key Laboratory of Biomimetic Robotics and Intelligent Systems; they are also with Guangdong Provincial Key Laboratory of Human-Augmentation and Rehabilitation Robotics in Universities, Department of Mechanical and Energy Engineering, Southern University of Science and Technology (SUSTech), Shenzhen, 518055, China. *Corresponding author: jiazz@sustech.edu.cn.

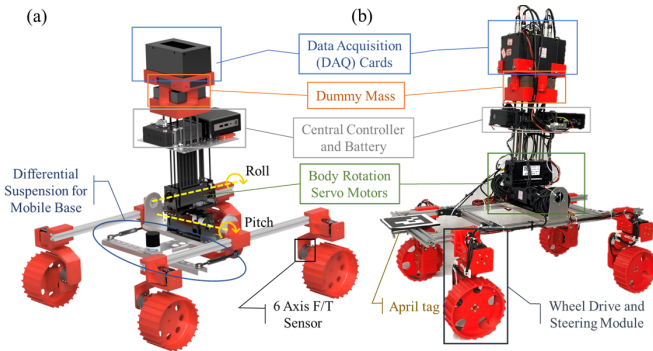


Fig. 1. Our first generation rover has a 4WD-4WS mobile base and a 2-DOF (roll and pitch) body-rotating mechanism. Note that the actual rover (b) used in experiments does not have suspension, because the 3D-printed suspension connectors in the original design (a) are not strong enough.

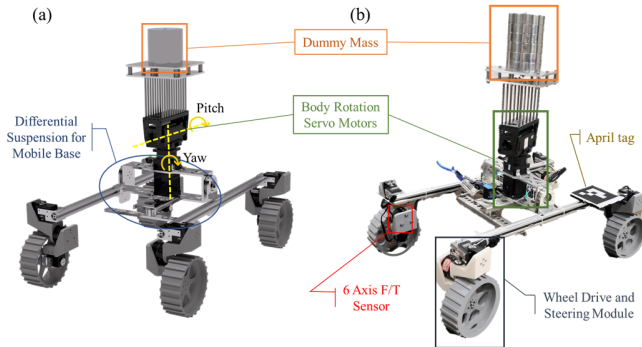


Fig. 2. Our second generation rover also has a 4WD-4WS mobile base (with differential suspension) and a 2-DOF (yaw and pitch) body-rotating mechanism. (a) CAD design. (b) The actual rover. To simplify the study, we place the DAQ cards, computer, and battery off-board (i.e., tethered).

II. ROBOT PLATFORM WITH BODY ROTATIONAL MASS-MOVING MECHANISM

A. Configuration of the Robot Platform

As shown in Figs. 1 and 2, we have developed two generations of wheeled rover platform with body-rotating mechanism for improved slope mobility studies. Both robots are composed of the main body, a mass-moving mechanism, and a mobile base with differential suspension. For the first generation rover, its main body includes the data acquisition (DAQ) cards for the F/T sensors, computer, battery, on-board sensors, and dummy mass that is used to emulate the scientific payload, antenna, and solar panels in an actual rover. Its 2-DOF (degree of freedom) body-rotating mechanism can control the roll and pitch angles of the main body. Hence, it can modulate the rover's COM and the load distributions on each wheel. For the second generation, its body-rotating mechanism controls the yaw and pitch angles of the main body. To simplify the design, the DAQ cards, computer, and battery are placed off-board (i.e., the power and controls are tethered); we use dummy mass to emulate these payload.

For both generation rovers, the mobile base has a four-wheel-drive and four-wheel-steering (4WD-4WS) configuration; this is similar to our previous work [8] [9]. The mobile base has four sets of wheel drive and steering modules that control the traveling speed and steering angle of each wheel. These modules are driven by networked servo motors that

are capable of both current and position control. For each module, the driving axis and steering axis intersect at the wheel center; this simplifies the rover control. The 6-axis F/T sensor measures the wheel load, drawbar pull, lateral forces, and driving torque of each wheel.

As shown in Fig. 1 and Fig. 2, the mobile base has a differential. Compared to the differential gear design in our previous work [9], we borrow the idea from NASA Mars Rover to make the suspension stronger. The differential is located under the main body (opposite to NASA design) so that it will not cause interference with the body-rotating mechanism during adjustment. An encoder is used to measure and calculate the relative angles of the left and right suspension arms with respect to the rover's main body. This differential helps to balance the wheel contacts when traveling on uneven terrains. Even when traveling on flat ground, it also helps to balance the uneven wheel loads caused by different wheel sinkages. It should be noted that the 3D-printed suspension connectors (between the rocker arm and cross-rod bearings) in our first generation prototype are not strong enough; hence, we reconfigure it into a non-suspension design for the actual experiments. Nevertheless, this compromise does not affect the experiment too much. We do not have this issue in our second generation rover.

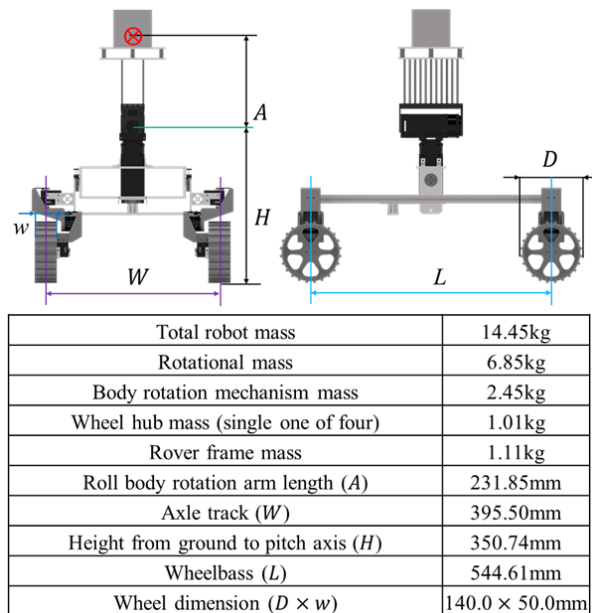


Fig. 3. Specifications of our second generation rover.

B. Body-Rotating Mechanism

An important feature of this research is the effective use of body-rotation mechanism to change the main body posture and rover's COM. This helps to even the wheel load distribution and improve the rover mobility over sandy slopes. As discussed in Section I-A, there are many related work on adjusting the COM for enhanced rover mobility, such as using linear actuators [2] [3] and rolling actuators [4] to adjusting the active suspension arms, using individual suspension [6] or wheel-leg mechanism [5] to achieve hybrid

locomotion modalities. These studies do not use the main body, which accounts for most of the robot weight, for mass-shifting purposes. Inspired by [7], we take full advantage of the large body weight for mass-moving purposes by using 2-DOF body-rotating mechanisms.

As shown in Fig. 1, in our first generation design, we adjust the roll and pitch angles of the main body by two servo motors (max torque: 40Nm). Compared to the highly integrated (including differential, worm gearboxes, motors, and encoders) and very complicated design in [7], our design has lower backlash and does not require such involved customization; it is more suitable for rapid prototyping purposes. Note that the differential gear design in [7] might not be suitable for large rovers. In contrast, our design separates the differential and body-rotating mechanism; it scales well with rover size and is more convenient for maintenance.

As shown in Fig. 2, our second generation rover uses a different design. The body-rotating mechanism is more like a robot arm with a waist joint and a should joint. We can adjust the COM distribution (its projection on the slope surface) through active control of the joint angles. For future real applications, this rover design resembles wheeled excavator that includes a wheeled platform (with suspensions) and a beefy excavator arm (with loaded terrain samples) that can effectively adjust the COM of the entire system.

In the sequel, we mainly focus on the second generation rover, studying its mechanics, control strategy, and mobility performance over sandy slopes. The first generation rover can be investigated in a similar way.

III. MECHANICS ANALYSIS AND CONTROL STRATEGY

A. Mechanics Analysis for Body-Rotation Mechanism

The rover has a 2-DOF rotational mechanism where the joint angles γ_1 and γ_2 can be adjusted to rotate rover's body (see Fig. 5). Based on the feedback information of slope (such as slope angle) sampled by on board sensors, the rover can even each wheel's loads by adjusting posture. The core of this process to even wheels' loads is adjusting COM's position. As shown in Fig. 4, we can achieve the different COM positions by adjusting the angles of the rotational mechanism(i.e., γ_1 and γ_2).

As shown in Fig. 5, we focus on slope climbing and traversing of the rover. For slope climbing, the wheel loads can be calculated from Eq. 1 and Eq. 2:

$$F_U = \frac{l_1 \cos(\theta) - h \sin(\alpha)}{L \cos(\alpha)} * Mg \quad (1)$$

$$F_D = \frac{(L - l_1) \cos(\theta) + h \sin(\alpha)}{L \cos(\alpha)} * Mg \quad (2)$$

For slope traversing, we can get corresponding results by swapping $\{L, l_1\}$ by $\{W, w_1\}$ in Eq. 1 and Eq. 2.

B. Wheel-Soil Interaction Mechanics

To better describe rover's mobility on sandy slope, we adopt the definition of slip angle β and slip ratio ($s > 0$) as below:

$$\begin{cases} s = 1 - \frac{v_x}{\omega r} \\ \beta = \tan^{-1} \left(\frac{v_y}{v_x} \right) \end{cases} \quad (3)$$

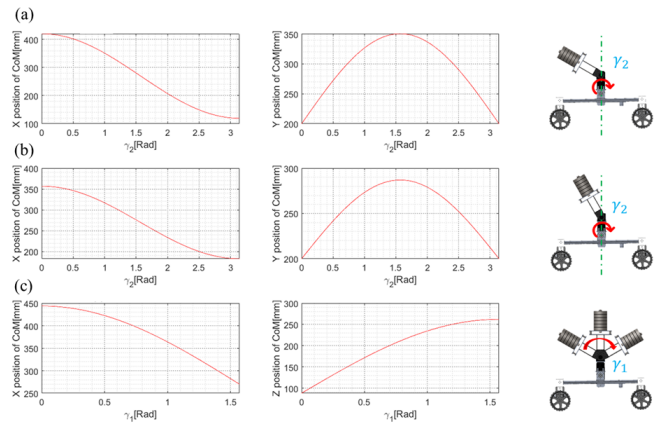


Fig. 4. Center of mass (COM) distribution by adjusting γ_2 and fixing γ_1 to 30° and 60° (see subfigure a and b). Subfigure c is the result when changing γ_1 and fixing γ_2 to 0° . The axis where the COM is not changed is not plotted. All the COM position is represented in world frame $\{W\}$ as shown in Fig. 5 with θ be 0° .

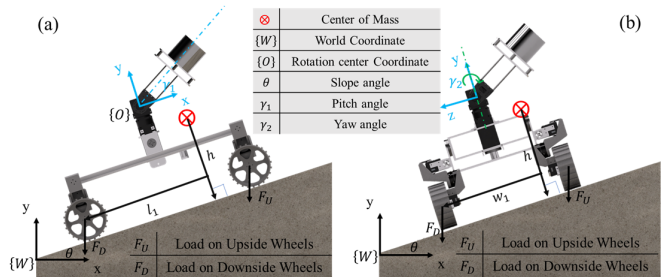


Fig. 5. Slope climbing (a) and slope traversing (b) maneuvers.

Adjusting rover's posture (changing rover's COM position) to even wheels loads is a widely used strategy to improve rover's mobility (see ref. [4]). Based on previous work, an integrated mode can be adopted to describe rover's posture (wheel loads) and slip angle and ratio. For more details, interested reader can see ref. [3], [10], etc. Learn from those integrated modes(see ref. [11]), we can adjust wheel loads by adjusting rover's mass-moving mechanism to meet better mobility on sandy slope.

C. Control Strategy for Sloped Motion

Based on the above modeling and analysis, we propose a rover attitude control strategy based on slope angle and optional feedback information of each wheel loads. The general idea of the strategy is to obtain slope angle in advance through sensors such as LiDAR and RGBD camera. Then we can calculate the rotation angle to balance the loads of four wheels, and drive the body-rotating mechanism to rotate to corresponding angles. If equipped with on board F/T(Force-and-Torque) sensors as feedback, the rotation angles can be dynamically adjusted. The control strategy is shown as Algorithm 1.

Algorithm 1 Attitude control strategy for slope traversing and climbing

- 1: **Input** : the slope angle α , rover motion direction (θ_b).
 - 2: **Output** : the rotate angle γ_1 and γ_2 .
 - 3: **Begin** :
 - 4: Estimate desired COM P_d with slope angle α and rover motion direction (θ_b).
 - 5: Resolve rotational angle γ_1 and γ_2 .
 - 6: **Optional** :
 - 7: Get 6 axis F/T data M_i .
 - 8: Update rotate angle γ_1 and γ_2 .
 - 9: **return** desired rotational angle γ_1 and γ_2 .
-

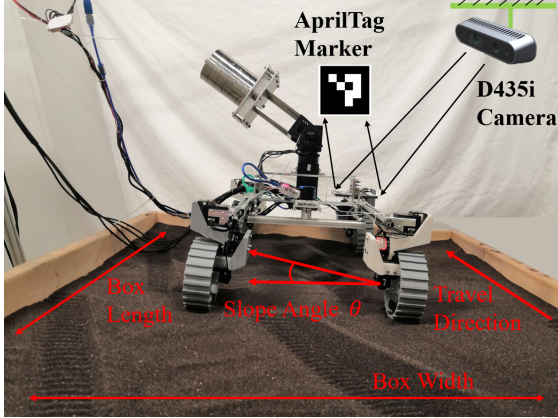


Fig. 6. Experiments of rover mobility over sandy slopes.

IV. EXPERIMENTS AND MOBILITY PERFORMANCE EVALUATION OVER SANDY SLOPES

A. Experiment Setup

1) *Experiment condition*: As shown in Fig. 6, the sand box (size: 1.2m*1m) is covered with 10cm loose sand. We use a hydraulic jack to adjust the inclination angle of the slope, and use an inclinometer to measure the actual slope angle. We use a Realsense D435i camera mounted on the rover platform. Then, we can calculate the actual spatial trajectory and the velocity of the rover. Each wheel is installed with a 6-axis F/T sensor that can feed the wheel forces back to the computer for control purposes.

2) *Experiment design*: In our experiments, the differential helps to balance the wheel contacts and load force differences when dealing with uneven terrains or different wheel sinkages. We also lock the steering motors and set zero steering angles during experiments. The reason is to minimize or isolate the influence of different factors on sloped mobility. In doing so, we can focus on the body-rotating mechanism. We investigate slope climbing and traversing maneuvers (Fig. 5), and use slip ratio, slip angle, drawbar pull, and wheel load to characterize the effectiveness of the proposed design, as shown in following figures. Under different slope angles, we conduct the same experiment three times and plot the results, including the mean value and standard deviations.

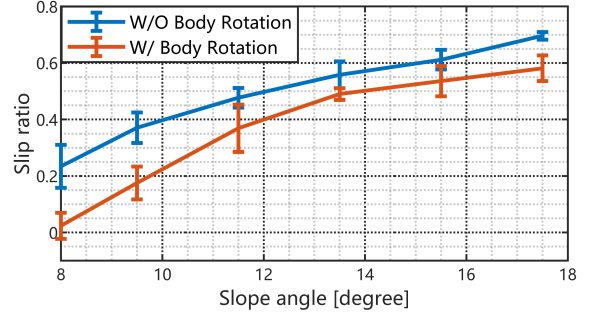


Fig. 7. Slip ratio versus slope angle during slope climbing.

B. Slope Climbing Results

During slope climbing, the effectiveness of the body-rotating mechanism can be demonstrated by comparing the slip ratio, drawbar pull, and force signals.

As shown in Fig. 7, the maximum slope angle the rover can successfully climbing without activating the body-rotating mechanism is 17.5°. Also, the slip ratio increases with the slope angle. When the rotating mechanism is activated, by adjusting the pitch angle of the main body and the wheel load, the slip ratio reduced under the same slope angle compared to the inactivated case. Also, the maximum slope angle the rover can overcome can be improved significantly when activating the mechanism; in fact, the rover is capable of climbing a 20° or a even deeper slope. In experiments, the maximum inclination angle of the sandbox is limited to 18° due to the placement of our hydraulic jack.

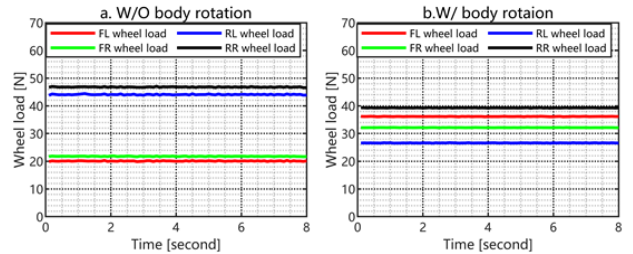


Fig. 8. Wheel loads in different driving state of the body-rotating mechanism during slope climbing (slope angle: 17.5°). The FL (front-left) and FR (front-right) wheels are on the upper-side, while the RL (rear-left) and RR (rear-right) wheels are on the down-side of the slope.

For 17.5° slope climbing, the wheel loads are given in Fig. 8. Note that the difference between the average wheel load of the front and rear wheels is about 22N when the rotating mechanism is not activated. This difference can be significantly reduced when we active the rotating mechanism. It should be pointed out that the result in Fig. 8(b) is preliminary; it can be greatly improved in our future studies. We know that the rear wheel load is much larger than the front wheel load during slope climbing. Consequently, the stress underneath the rear wheel will exceed the supporting limit of the terrain, causing significant slippage and sinkage and the eventual immobility. In contrast, as shown in Fig. 5(a), when we adjust the pitch angle of the body-rotating mechanism,

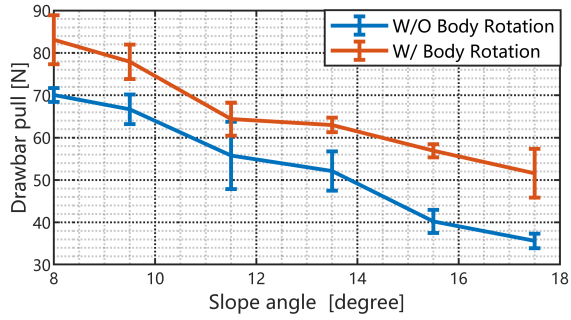


Fig. 9. Drawbar pull during slope climbing.

we can balance the wheel load and driving torque, and effectively mitigate the slippage and sinkage problems.

To further evaluate the climbing performance, we add another set of experiments, by measuring the standstill drawbar pull (i.e., traction force). As shown in Fig. 9, the rover drawbar pull reduces with the slope angle. This is because the down-hill component of the gravity that the traction motor need to overcome will increase with the slope angle. We see that we can significantly improve the rover's traction performance by active control of the body-rotating mechanism, as shown in Fig. 9. This is because we can achieve even wheel load distribution and similar wheel sinkages, thereby avoiding wheel stall or excessive wheel slippages that can significantly reduce the wheel traction force.

C. Slope Traversing Results

For slope traversing, the effectiveness of the body-rotating mechanism can be demonstrated by comparing the slip ratio, slip angle, and force signals.

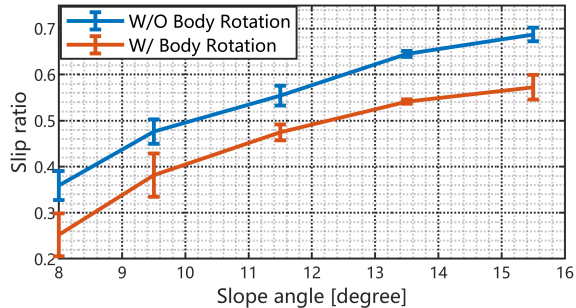


Fig. 10. Slip ratio versus slope angle during slope climbing.

As show in Fig. 10, the slip ratio increases with the slope angle during slope traversing experiments for both driving modes. We see that the slip ratio can be reduced (by about 0.1) when activating the body-rotating mechanism, compared with the inactivation mode.

Similar to the climbing task, the key for improved slope traversing is also adjusting the rover COM and wheel load distributions according to the terrain and the wheel forces (measured by the F/T sensor) (see [12]). The wheel load shown in Fig. 11 is measured on a 15.5° slope. We see that

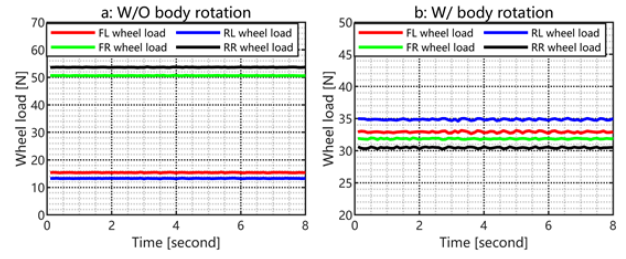


Fig. 11. Wheel load in different driving states while traversing slope. FL and RL wheels are on slope upside, FR and RR wheels are on slope downside. The wheel load is measured on 15.5° slope.

the difference between the upper-side wheel loads and the downside wheel loads is about $34N$ in the inactivation mode. In contrast, this difference can be reduced to less than $5N$ when activating the rotating mechanism.

It should be noted that there is apparent difference in the body-rotating adjustment process during slope traversing and slope climbing tasks. When the rotating mechanism is not activated, the rover wheel base is large than the axle track ($L > W$, see Fig. 4), the COM of the main body is much closer to the downhill side wheel during slope traversing compared to slope climbing. Hence, the load difference between upper-side and downside wheels is larger in slope traversing. When we activate the body-rotating mechanism, because rover geometry configuration ($L > W$), it is easier to adjust the COM of the main body outside the supporting polygon of the rover wheels during slope traversing; however, this is not the case for slope climbing. Therefore, the body-rotating mechanism has larger control authority in slope traversing tasks compared to slope climbing case.

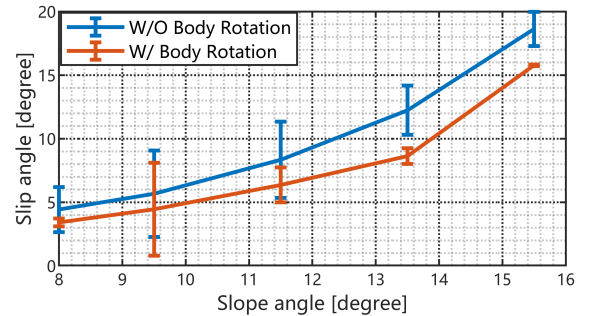


Fig. 12. wheel load in different driving state while traversing slope.

From Fig. 12, we see that the rover slip angle increases with the slope angle. This is because the shearing force that the slope can provide is limited. The downhill gravity force components of each wheel increases with the slope angle. When this downhill force exceed the terrain limit, the slip angle will have a significant increase. The body-rotating mechanism can reduce the slip angle during slope traversing, however, this reduction is limited. This is mainly because the mobile platform is parallel to the slope surface (see [13]). Although we can adjust the rover COM and wheel load through body-rotating mechanism, we cannot change

the contact pose between the wheel and slope surface. Hence, we cannot have better shearing force along the slope surface.

V. CONCLUSIONS AND FUTURE WORK

In this paper, we developed two generations of rover prototypes consisting of a 4WD-4WS mobile base with differential suspension, and a 2-DOF body-rotating mass-moving mechanism for improved slope mobility. Based on mechanics analysis and terramechanis models, we developed an associated control strategy for the body-rotating mechanism. This control strategy can adjust the pose of the main body when given the slope angle and traveling direction. We evaluated the off-road sloped mobility of the proposed design and control strategy through experimental studies of slope traversing and climbing tasks.

In the future, we will improve our rover design. One limitation of current design (also literature [7]) is that the body is too tall; it is not compact. We plan to use scissor-lift or sliding mechanism to control the height of the main body for a more compact design. An important future work is improved control strategy, including: (1) use on-board perception system to estimate the slope angle; (2) combine with wheel steering control; (3) integrate the body-rotating control with the path planning module, for optimal whole-body motion planning.

ACKNOWLEDGMENTS

This work was supported in part by the Science, Technology and Innovation Commission of Shenzhen Municipality under grant no. ZDSYS20200811143601004.

REFERENCES

- [1] K. Iagnemma and S. Dubowsky, *Mobile robots in rough terrain: Estimation, motion planning, and control with application to planetary rovers*. Springer Science & Business Media, 2004, vol. 12.
- [9] —, “Fast analytical models of wheeled locomotion in deformable terrain for mobile robots,” *Robotica*, vol. 31, no. 1, p. 35, 2013.
- [2] H. Inotsume, M. Sutoh, K. Nagaoka, K. Nagatani, and K. Yoshida, “Slope traversability analysis of reconfigurable planetary rovers,” in *2012 IEEE/RSJ International Conference on Intelligent Robots and Systems*, 2012, pp. 4470–4476.
- [3] H. Inotsume, M. Sutoh, K. Nagaoka, K. Nagatani, and K. Yoshida, “Modeling, analysis, and control of an actively reconfigurable planetary rover for traversing slopes covered with loose soil,” *Journal of Field Robotics*, vol. 30, no. 6, pp. 875–896, 2013.
- [4] D. Wettergreen, S. J. Moreland, K. Skonieczny, D. Jonak, D. Kohanbash, and J. Teza, “Design and field experimentation of a prototype lunar prospector,” *International Journal of Robotics Research*, vol. 29, no. 12, pp. 1550 – 1564, October 2010.
- [5] F. Cordes, C. Oekermann, A. Babu, D. Kuehn, T. Stark, F. Kirchner, and D. Bremen, “An active suspension system for a planetary rover,” in *Proceedings of the International Symposium on Artificial Intelligence, Robotics and Automation in Space (i-SAIRAS)*, 2014, pp. 17–19.
- [6] S. Shrivastava, A. Karsai, Y. O. Aydin, R. Pettinger, W. Bluethmann, R. O. Ambrose, and D. I. Goldman, “Material remodeling and unconventional gaits facilitate locomotion of a robophysical rover over granular terrain,” *Science Robotics*, vol. 5, no. 42, 2020.
- [7] B.-S. Sim, K.-J. Kim, and K.-H. Yu, “Development of body rotational wheeled robot and its verification of effectiveness,” in *2020 IEEE International Conference on Robotics and Automation (ICRA)*. IEEE, 2020, pp. 10405–10411.
- [8] Z. Jia, W. Smith, and H. Peng, “Terramechanics-based wheel-terrain interaction model and its applications to off-road wheeled mobile robots,” *Robotica*, vol. 30, no. 3, p. 491, 2012.
- [10] H. Inotsume, M. Sutoh, K. Nagaoka, K. Nagatani, and K. Yoshida, “Evaluation of the reconfiguration effects of planetary rovers on their lateral traversing of sandy slopes,” in *2012 IEEE International Conference on Robotics and Automation*. IEEE, 2012, pp. 3413–3418.
- [11] L. Ding, Z. Deng, H. Gao, J. Tao, K. D. Iagnemma, and G. Liu, “Interaction mechanics model for rigid driving wheels of planetary rovers moving on sandy terrain with consideration of multiple physical effects,” *Journal of Field Robotics*, vol. 32, no. 6, pp. 827–859, 2015.
- [12] J.-Y. Wong and A. Reece, “Prediction of rigid wheel performance based on the analysis of soil-wheel stresses part i. performance of driven rigid wheels,” *Journal of Terramechanics*, vol. 4, no. 1, pp. 81–98, 1967.
- [13] G. Ishigami, A. Miwa, K. Nagatani, and K. Yoshida, “Terramechanics-based model for steering maneuver of planetary exploration rovers on loose soil,” *Journal of Field robotics*, vol. 24, no. 3, pp. 233–250, 2007.